# Photoemission spectra from conduction bands and core levels of sputter-deposited tantalum films

Claude M. Penchina*
*Department of Physics and Astronomy, University of Massachusetts, Amherst, Massachusetts 01002* †
*and Max-Planck-Institut für Festkörperforschung, Stuttgart, Federal Republic of Germany*‡
(Received 22 December 1975)

Photoemission spectra of tantalum films, deposited by dc sputtering onto a room-temperature substrate, were obtained using a monochromatized aluminum x-ray source (Al $K\alpha_{1,2}$—1486.6 eV) and a helium uv resonance lamp (HeI—21.2 eV, and HeII—40.8 eV). The x-ray photoemission spectra (XPS) were used to determine the density of electron states in the conduction band, the core-level binding energies, the spin-orbit splitting, and the chemical shift due to surface contamination. The much higher resolution ultraviolet photoemission spectra (UPS) were used to improve resolution of the conduction-band density of states near the Fermi level and to determine the work function. UPS data were also used to precisely calibrate the XPS energies. Comparison with similar experiments on tungsten indicate that the conduction bands are consistent with a rigid-band model.

## I. INTRODUCTION

The band structure of bcc crystalline tantalum has been calculated by Petroff and Viswanathan[1,2] using the augmented-plane-wave (APW) method.[3] The qualitative similarity of the bands to those calculated for tungsten[1,2,4–7] and molybdenum[1,2] is taken by them as a theoretical justification of the rigid-band model for body-centered transition metals. (In Sec. IV, we present an experimental justification.)

The free-atom electronic configuration $(5d)^3(6s)^2$ was used to construct the potential. There are five conduction electrons per atom. The computations show the first conduction band to begin 4.1 eV above the bottom of the muffin-tin potential and to consist mainly of 6*s* orbitals; the 5*d* band begins 1.4 eV higher; the Fermi level is 5.5 eV above the bottom of the conduction bands.

Previously, photoemission spectra on sputter-deposited tungsten films[8] indicated a density of electron states in the conduction band in qualitative agreement with a smeared out version of the band-structure calculations. In this paper, we describe similar measurements of x-ray-induced (XPS) and uv-induced (UPS) photoemission spectra of sputter-deposited tantalum films.

## II. EXPERIMENT

Monochromatized XPS measurements were performed with a vacion-pumped Hewlett-Packard 5950 ESCA spectrometer. UPS and nonmonochromatized XPS measurements were performed with a liquid-nitrogen trapped, oil diffusion pumped, Vacuum Generators ESCA III system.

Samples (~0.5 μm thick) were prepared inside a sample preparation chamber (turbomolecular pumped, base pressure $10^{-7}$ Torr) by diode sputtering of tantalum onto a stainless-steel substrate at room temperature in an argon atmosphere ($10^{-6}$ purity) at $(2-3)\times10^{-2}$ Torr with a dc current of ~1 mA at 2300 V. The argon was pumped out and, without breaking the vacuum, the sample was moved to the analyzer chamber where it was maintained in ultrahigh vacuum (better than $2\times10^{-9}$ Torr) throughout the measurements. The sputtering target was a 0.005-in.-thick metallurgical-grade tantalum foil obtained from Norton Metals Div., Newton, Mass.

Tantalum films prepared by dc argon-ion sputtering in clean vacuum systems onto room-temperature substrates are known to consist mainly of tetragonal β – Ta ($a=5.3$ Å, $c=9.9-10$ Å) with some bcc α – Ta ($a_0=3.3$ to 3.4 Å).[9]

## III. RESULTS

### A. Sensitivity to surface contamination

XPS data on photoelectrons from the $N$ VI-VII($4f_{5/2\text{-}7/2}$) spin-orbit split doublet are shown in Fig. 1. The photoelectron energy distributions show binding energies of $22.5\pm0.1$ eV and $24.35\pm0.1$ eV for the $N$ VII and $N$ VI levels, respectively; the spin-orbit splitting is $1.85\pm0.1$ eV. The apparent $N$ VII/$N$ VI peak height ratio is 6.3/6 for the cleanest sample [Fig. 1(a)]. The data, however, show the usual rising background of inelastically scattered electrons following the onset of sharp spectra from the core levels. Subtracting this inelastic background for the cleanest sample, Fig. 1(a), the $N$ VII/$N$ VI intensity ratio is 7/6; this is fairly close to the theoretical degeneracy ratio of 8/6.

Figures 1(b)–1(d) show the effects of surface contamination by residual gases in the vacuum

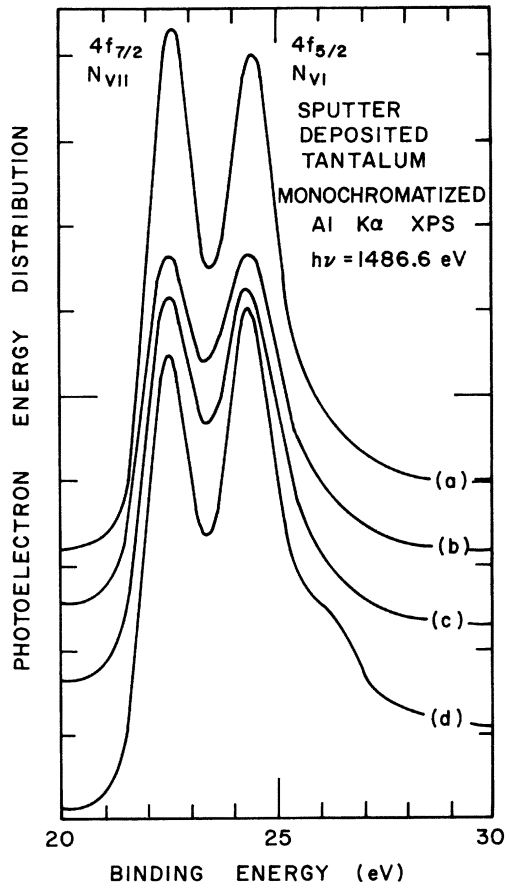


FIG. 1. Energy distribution curves for electrons excited from the $N$VI and $N$VII core levels of sputter-deposited tantalum by monochromatized Al$K\alpha_{1,2}$ x rays for increasing levels of contamination. The energy scale is photon energy minus measured photoelectron energy relative to $E_F$ as reference. For unscattered photoelectrons, this corresponds to the binding energy (below $E_F$) of the initially filled electron states. Curves are offset vertically for clarity. Apparent $N$VII/$N$VI ratio is: (a) 1.05, (b) 1.00, (c) 0.98, (d) 0.91 (see text).

system on the $N$VI-$N$ VII core level spectra. We characterize the contamination by the apparent $N$ VII/$N$ VI peak height ratio, i.e., the ratio obtained without subtracting the inelastic background; this apparent ratio varies from 1.05 in our cleanest sample [Fig. 1(a)] to 0.91 [Fig. 1(d)]. With increasing contamination a shoulder grows on the side of higher binding energy, emerging as a very slight peak at 26.3-eV binding energy; this is accompanied by an increase in the 24.35-eV peak and a decrease of the 22.5-eV peak. There is no noticeable shift in either the $N$ VI or $N$ VII binding energies, although there is some very slight broadening of the $N$ VI spectral peak.

The behavior of the curves in Figs. 1(a)–1(d) is explained as due to a 1.95 ± 0.2-eV chemical shift due to surface oxidation of the tantalum. The 1.95-eV shifted $N$ VII line from the oxidized tantalum overlaps the $N$ VI line of pure tantalum. The oxidation thus increases the height of the 24.35-eV peak at the expense of the 22.5-eV peak. The lack of perfect overlap between the 1.95 ± 0.2-eV chemical shift and the 1.85 ± 0.1-eV spin-orbit splitting causes the slight broadening of the 24.35-eV peak. The lack of shift of either the main $N$ VI or $N$ VII lines indicates that the core level binding energies determined by XPS are quite reliable, even in the presence of considerable surface contamination.

Figures 2, 3, and 4 show the effects of surface contamination on the spectra of electrons photoemitted from the conduction bands in UPS (21.2 and 40.8 eV) and XPS (1486.6 eV), respectively. Figures 2 and 3 demonstrate that, especially in the region beyond 4-eV binding energy, the UPS spectra are extremely sensitive to surface contamination; we were unable to obtain samples sufficiently clean to get reliable reproducible photoelectron spectra beyond 4-eV binding energy. By contrast, for the first few eV, the spectral shape of the He II (40.8-eV) UPS photoelectron distribution is reproducible, and not very sensitive to surface contamination. Figure 4 shows that the major effect of contamination on the XPS conduction-band spectra occurs as a slight shift of signal strength, from the main peak to a weak broad peak in the region beyond 4-eV binding energy. This weak broad peak in Fig. 4(b) is quite small compared with the ones in UPS. Thus, the curve for the cleaner

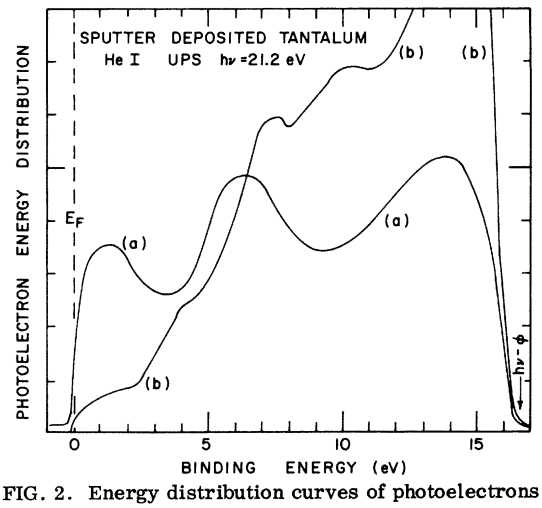


FIG. 2. Energy distribution curves of photoelectrons from sputter-deposited tantalum excited by He I uv source. The energy scale is photon energy minus measured photoelectron energy relative to $E_F$ as a reference. For unscattered photoelectrons, this corresponds to the binding energy (below $E_F$) of the initially filled electron states. Apparent $N$VII/$N$VI ratio is: (a) 0.99, (b) 0.90 (see text).

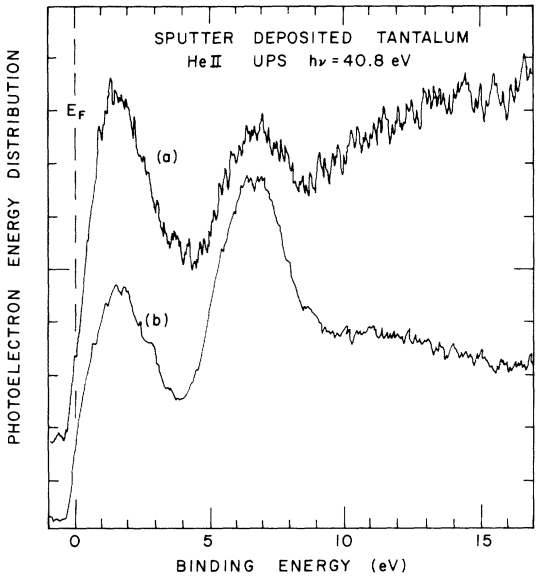


FIG. 3. Energy distribution curves of photoelectrons from sputter-deposited tantalum excited by He II uv source. The energy scale is photon energy minus measured photoelectron energy relative to $E_F$ as reference. For unscattered photoelectrons, this corresponds to the binding energy (below $E_F$) of the initially filled electron states. Curves are offset vertically for clarity. Apparent $N_{VII}/N_{VI}$ ratio is: (a) 1.03, (b) 0.99 (see text).

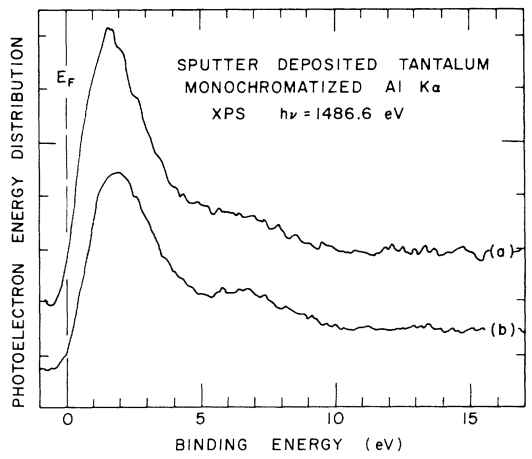


FIG. 4. Energy distribution curves of photoelectrons from sputter-deposited tantalum excited by monochromatized Al $K\alpha_{1,2}$ x rays. The energy scale is photon energy relative to $E_F$ as reference. For unscattered photoelectrons, this corresponds to the binding energy (below $E_F$) of the initially filled electron states. Curves are offset vertically for clarity but have the same vertical sensitivity. Apparent $N_{VII}/N_{VI}$ ratio is (a) 1.05, (b) 0.98 (see text).

sample of Fig. 4(a) is a good representation of the conduction-band XPS spectrum of pure tantalum.

The trend of sensitivity to surface contamination is similar to that which we observed previously in tungsten.[8] It is to be expected because the escape depth of the x-ray excited high-energy photoelectrons is much larger than that of the uv excited low-energy photoelectrons,[10,11] and because the oxygen $L$ shell has a rather large cross section for excitation by uv photons.[12]

### B. Density of conduction states

From a critical examination of Figs. 2–4, we can put together a composite picture of an empirical density of states for the conduction band below the Fermi level $E_F$. We start with a discussion of states near $E_F$ and then move in the direction of tighter binding.

For the first 4 eV below $E_F$, the He II UPS spectra are essentially independent of oxygen contamination, and are of high resolution (0.2 eV). The electronic states involving the oxides, as a rule, lie 3–5 eV deeper in energy. In general, one would expect some influence of the available final states density on the UPS spectra. However, previous experience indicates that this is not usually very important for He II excitation.[8]

By fitting the high resolution (0.1 eV for He I, 0.2 eV for He II) UPS data with the lower resolution (0.5 eV) monochromatized XPS data over the first 4 eV, we calibrate the position of the Fermi level in XPS with the precision (0.1–0.2 eV) of the UPS data.[8,13] We also use this comparison to sharpen the XPS data near the Fermi level. We then subtract the rising background of inelastically scattered electrons from the XPS data to obtain the energy distribution of primary photoelectrons.

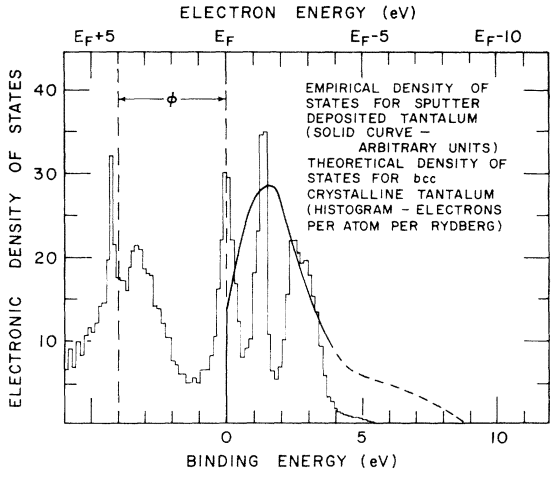


FIG. 5. Curve is the empirical density of states for sputter-deposited tantalum deduced from our UPS and XPS measurements. The histogram is a theoretical density of states for bcc crystalline tantalum from Petroff (Ref. 2). The energy scale is binding energy below $E_F$.

This is presumed to reflect the density of filled states below the Fermi level.[8] We designate it as the empirical density of states[8] and plot it in Fig. 5 together with a theoretically computed density of states.[2]

### C. Core levels

The core level energies determined by monochromatized XPS are tabulated in Table I. The designation of the states is determined by comparison with the tabulation of Bearden and Burr.[14] The difference between our XPS levels and those tabulated by Bearden and Burr vary widely, but have a mean value of 2.0 eV. This should not be regarded as a "chemical" shift due to the difference between sputter-deposited and crystalline tantalum. Much of the mean shift may be due to the use of an incorrect carbon calibration line by Bearden and Burr, and/or possible surface contamination of their samples.[8] It is (within the uncertainties) similar to the 1.5-eV mean shift found between the XPS core level energies of sputter-deposited tungsten and the values tabulated by Bearden and Burr for crystalline tungsten. This is discussed further by Penchina *et al.*[8] It is perhaps surprising that Bearden and Burr did not resolve the $1.85 \pm 0.1$-eV spin-orbit splitting of the $N$ VI-$N$ VII doublet.

The nonmonochromatized XPS data show broad structure around 167 and 180 eV emitted electron energy, as shown in Fig. 6. These energies agree well with the Auger transitions at 166 and 179 eV reported by Palmberg *et al.*,[15] and those at 168 and 181 eV reported by Haas *et al.*[16] These Auguer lines have been identified as $N_5N_6N_6$ and $N_4N_{6,7}N_{6,7}$, repectively, by Chung and Jenkins.[17] (This identification appears to be the most reliable although others have also been proposed. See Haas,[16] Strausser,[18] Clarke.[19])

These Auger transitions are not noticed in the monochromatized XPS spectra. This is in part due to the unusual design of the Hewlett-Packard electron analyzer which actually broadens Auger spectra. It is designed to sharpen photoelectron spectra by undoing the dispersion of x rays (and hence photoelectron energies) across the sample caused by the dispersive x-ray monochromator. This, however, broadens Auger spectra, since Auger electron energies are independent of the exciting radiation,[20] and thus not dispersed across the sample. On the other hand, the resolution of the Vacuum Generators ESCA system is better for Auger electrons than for x-ray photoelectrons because for Auger it is not limited by the large linewidth of the Al $K\alpha_{1,2}$ radiation. However, the large width of the Auger lines as observed with the VG ESCA, indicates that the lack of these lines in the HP ESCA spectra could not be due to instrumental broadening alone.

### D. Work function

Figure 2 indicates that there is a cutoff in the He I (21.2 eV) photoelectron spectrum at a binding energy of 16.3 eV. This corresponds to electrons with energy 4.9 eV (21.2 −16.3 eV) above the Fermi energy, and thus to a work function of 4.9 eV. This is rather larger than the values of $4.1 \pm 0.1$ eV quoted in the *Handbook of Chemistry and Physics*.[21]

## IV. DISCUSSION

### Rigid-band model

The photoemission data for conduction electrons with binding energy greater than 4 eV seemed to

TABLE I. Binding energies for crystalline tantalum tabulated by Bearden and Burr (Ref. 14), and for sputter-deposited tantalum from our experiments. The shift, i.e., the difference between these two tabulations of core level energy is listed in the right-hand column. See text and Ref. 8 for discussion of the reliability of these shifts.

| Core level | bcc crystalline tantalum binding energy Bearden and Burr (Ref. 14) (eV) | Sputter-deposited tantalum binding energy (eV) | Shift (eV) |
|---|---|---|---|
| $N$ I $4s$ | $565.5 \pm 0.5$ | $563.9 \pm 1.0$ | $1.6 \pm 1.5$ |
| $N$ II $4p_{1/2}$ | $464.8 \pm 0.5$ | $463.4 \pm 0.6$ | $1.4 \pm 1.1$ |
| $N$ III $4p_{3/2}$ | $404.5 \pm 0.4$ | $401.5 \pm 0.6$ | $3.0 \pm 1.0$ |
| $N$ IV $4d_{3/2}$ | $241.3 \pm 0.4$ | $238.5 \pm 0.5$ | $2.8 \pm 0.9$ |
| $N$ V $4d_{5/2}$ | $229.3 \pm 0.3$ | $226.9 \pm 0.3$ | $2.4 \pm 0.6$ |
| $O$ I $5s$ | $71.1 \pm 0.5$ | $70.4 \pm 1.5$ | $0.7 \pm 2.0$ |
| $O$ II $5p_{1/2}$ | $44.9 \pm 0.4$ | $43.1 \pm 0.6$ | $1.8 \pm 1.0$ |
| $O$ III $5p_{3/2}$ | $36.4 \pm 0.4$ | $33.6 \pm 0.2$ | $2.8 \pm 0.6$ |
| $N$ VI $4f_{5/2}$ | $25.0 \pm 0.4$ | $24.35 \pm 0.1$ | $0.65 \pm 0.5$ |
| $N$ VII $4f_{7/2}$ | $25.0 \pm 0.4$ | $22.5 \pm 0.1$ | $2.5 \pm 0.5$ |

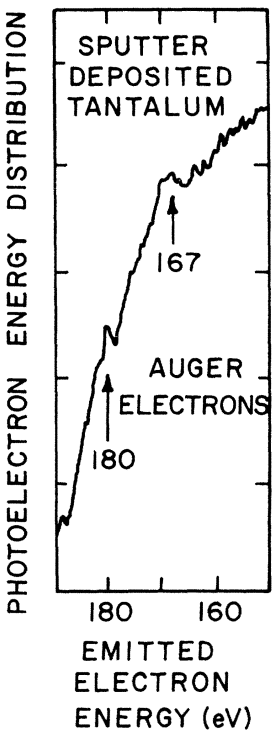


FIG. 6. Energy distribution curves of photoelectrons from sputter-deposited tantalum excited by nonmonochromatized Al $K\alpha_{1,2}$ x ray source. The energy scale is the emitted electron energy above $E_F$ as reference. The structure near 167 and 180 eV has been identified (Ref. 17) as corresponding to $N_5N_6N_6$ and $N_4N_{6,7}N_{6,7}$ Auger transitions, respectively.

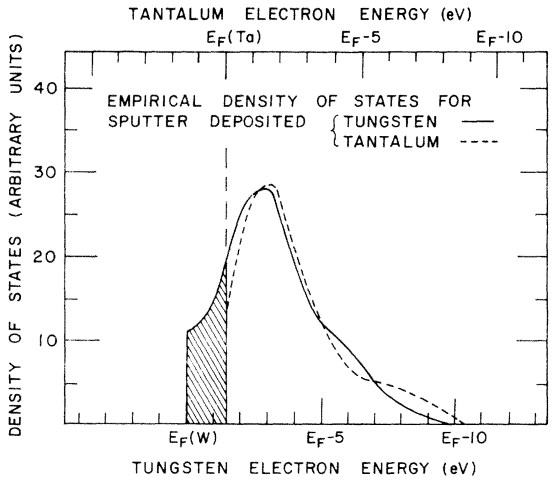


FIG. 7. Empirical density of states for sputter-deposited Ta and W (Ref. 8). The energy scales are initial electron energy relative to $E_F$ of the respective metals. For evaluation of the rigid-band model, $E_F$ of Ta is shifted to the energy below which $W$ has five conduction electrons per atom.

be sensitive to surface contamination. In Sec. III A, we presented arguments to show that the XPS data of our cleanest sample [Fig. 4(a)] are a good representation of the density of filled conduction-band states of pure tantalum. Still, in the region beyond 4 eV, where the density of states is small, even weak contamination effects could cause relatively large distortions in the photoelectron spectrum. Thus, as a precaution, this section of our empirical density of states curve is shown dashed in Fig. 5.

A comparison of our empirical density of states with the theoretical density of states of Petroff[1,2] might lead one to believe that much of the photosignal attributed to electrons with more than 4-eV binding is due to contamination. Our Fermi energy of 8.7 eV is much higher than the predicted 5.5 eV. The discrepancy, however, is more likely due to problems with Petroff's theoretical model than with the experiment. A comparison of the situation for tungsten is instructive here. The empirical density of states of sputter-deposited tungsten[8] shows a Fermi energy of 10 eV. This is in good agreement with the values predicted by the relativistic calculations of Loucks,[7] and with the $E_2$ calculation of Mattheiss,[4] which reduced the exchange interaction by 30%. It is much higher than 6.8 eV predicted for tungsten by Petroff[1,2] using nonrelativistic APW with full Slater exchange interaction.

It is also interesting now to compare the empirical density of states of tungsten and tantalum. Tungsten has six conduction electrons per atom, and tantalum only five. According to the rigid-band model,[22] the conduction band of tantalum should be very similar to that of tungsten, but only $\frac{5}{6}$ as many states filled. In Fig. 7 we show the empirical density of states of tungsten (solid curve) with the top $\frac{1}{6}$ of its states removed (cross-hatched area). The top of the remaining distribution is aligned with the Fermi level of tantalum, and the empirical density of states of tantalum drawn as a dotted curve in Fig. 7. The resemblance between these two curves is quite obvious, and at least as good as that between the theoretical density of states for tantalum and tungsten as computed by Petroff.[1,2]

We take this result as experimental evidence that (i) the rigid-band model is a reasonable approximation for the situation of sputter-deposited tungsten and tantalum; (ii) the empirical density of states of Fig. 5 is a good representation for clean tantalum; and (iii) Petroff's[1,2] standard nonrelativistic calculations with full Slater exchange consistently underestimate the Fermi energy.

## V. CONCLUSIONS

We have combined ultraviolet and x-ray induced photoelectron spectroscopy to obtain a high resolution empirical density of states for the conduction bands of sputter-deposited tantalum. This density of states qualitatively resembles a smeared version of the theoretical density predicted by Petroff,[1,2] but indicates a larger Fermi energy, 8.7 eV. Comparison of results with those for sputter-deposited tungsten provides an experimental verification of the value of the rigid-band model for these metals.

The binding energies of the core levels have been accurately determined (some within 0.1 eV) by means of monochromatized XPS measurements, calibrated by high resolution UPS measurements. A spin-orbit splitting of $1.85 \pm 0.1$ eV was resolved for the $N$ VI-$N$ VII ($4f_{5/2}$-$4f_{7/2}$) doublet. Although there were wide variations, the core level binding energies were less than those reported by Bearden and Burr[14] by a mean value of 2.0 eV.

We have seen that the effect of contamination by residual gases in the vacuum system on the photoelectron spectra of conduction electrons is to greatly increase the photo signal for conduction electrons bound more than 4 eV below the Fermi level. The effect on the core level XPS spectrum is the addition of weak satellites chemically shifted by $1.95 \pm 0.2$ eV to tighter binding.

## ACKNOWLEDGMENTS

We wish to thank G. Krutina and W. Neu for aid in performing the measurements. We wish to thank J. Lannin and P. Kemeny for some useful discussions and assistance, and N. Shevchik for his continued help and encouragement. The hospitality of M. Cardona and the other directors of the Max Planck Institut für Festkörperforschung was greatly appreciated. We thank J. Dudzik of the Norton Metals Division for her kind donation of the sputtering target.

---

*Supported in part by the U. S. NSF and by a partial travel grant from the University of Massachusetts.

† Permanent address.

‡ Experiments were performed while the author was at the Max Planck Institut.

[1] I. Petroff and C. R. Viswanathan, in *Electronic Density of States*, U. S. Natl. Bur. Stand. Spec. Pub. No. 323, edited by L. H. Benett (U. S. GPO, Washington, D. C., 1971), p. 53.

[2] I. Petroff and C. R. Viswanathan, Phys. Rev. B 4, 799 (1971).

[3] J. C. Slater, Phys. Rev. 51, 846 (1937); 81, 385 (1951).

[4] L. F. Mattheiss, Phys. Rev. 139, A1893 (1965).

[5] T. L. Loucks, Phys. Rev. 139, A1181 (1965).

[6] T. L. Loucks, Phys. Rev. 139, A1333 (1965).

[7] T. L. Loucks, Phys. Rev. 143, 506 (1966).

[8] G. M. Penchina, E. Sapp, J. Tejeda, and N. Shevchik, Phys. Rev. B 10, 4187 (1974).

[9] P. N. Baker, Thin Solid Films 14, 3 (1972).

[10] J. Tejeda, M. Cardona, N. J. Shevchik, D. W. Langer, and E. Schonherr, Phys. Status Solidi B 58, 189 (1973).

[11] I. Lindau and W. E. Spicer, J. Electron Spectrosc. Related Phenomena 3, 409 (1974).

[12] M. Cardona, J. Tejeda, N. J. Shevchik, and D. W. Langer, Phys. Status Solidi 58, 483 (1973).

[13] M. Cardona, C. M. Penchina, E. E. Koch, and P. Y. Yu, Phys. Status Solidi B 53, 327 (1972).

[14] J. Bearden and A. Burr, Rev. Mod. Phys. 39, 125 (1967); also in *Handbook of Chemistry and Physics*, 55th ed., edited by R. C. Weast (Chemical Rubber Co., Cleveland, Ohio, 1974—1975), p. E-189.

[15] P. W. Palmberg, G. E. Riach, R. E. Weber, and N. C. MacDonald, *Handbook of Auger Electron Spectroscopy* (Physical Electronics Industries, Edina, Minn., 1972).

[16] T. W. Haas, J. T. Grant, and G. J. Dooley, Phys. Rev. B 1, 1449 (1970).

[17] M. F. Chung and I. H. Jenkins, Surf. Sci. 22, 479 (1970).

[18] Y. Strausser and J. J. Uebbing, wall chart printed by Varian Associates (1971), also reprinted in Ref. 20.

[19] T. A. Clarke, R. Mason, L. Randaccio, and J. M. Thomas, J. Chem. Soc. Lond. A 9, 1156 (1971).

[20] C. C. Chang, in *Characterization of Solid Surfaces*, edited by P. F. Kane and G. B. Larrabee (Plenum, New York, 1974).

[21] R. C. Weast, editor, *Handbook of Chemistry and Physics*, 55th ed. (Chemical Rubber Co., Cleveland, Ohio, 1974–1975), p. E-82.

[22] E. A. Stern, Phys. Rev. 157, 544 (1967), and references therein.